Energy loss in calorimeters using muon spectrometer information at the 2004 ATLAS Combined Test Beam

Avolio, G.
Università della Calabria

Cerutti, F., Pontecorvo, L.
Istituto Nazionale di Fisica Nucleare

Abstract

In 2004 an ATLAS Combined Test Beam (CTB) was performed in the CERN North area. A complete slice of the barrel detector and of the muon end-cap was tested to study the combined detector performance. In this note we present an analysis of the muon energy loss in the Liquid Argon and Tile calorimeters and its correlation with the momentum measured with the MDT detectors for muons deflected by a dipole magnet in the range $100 - 350\ GeV$.

ATL-MUON-PUB-2008-001
3 January 2008

Contents

1 Introduction

The 2004 Combined Test Beam [1] (Figure 1) offered the first opportunity to acquire data from various ATLAS detectors at the same time. The CTB included elements of all the sub-detectors of the ATLAS Barrel − the Inner Detector (Pixel, SCT, TRT), the electromagnetic calorimeter (LAr), the hadronic calorimeter (Tilecal), the muon system (MDT and RPC) − as well as elements of the muon end cap system (MDT, TGC and CSC). In the followings a brief description of the muon and calorimeter detectors, which will be the subjects of the whole work, is given.

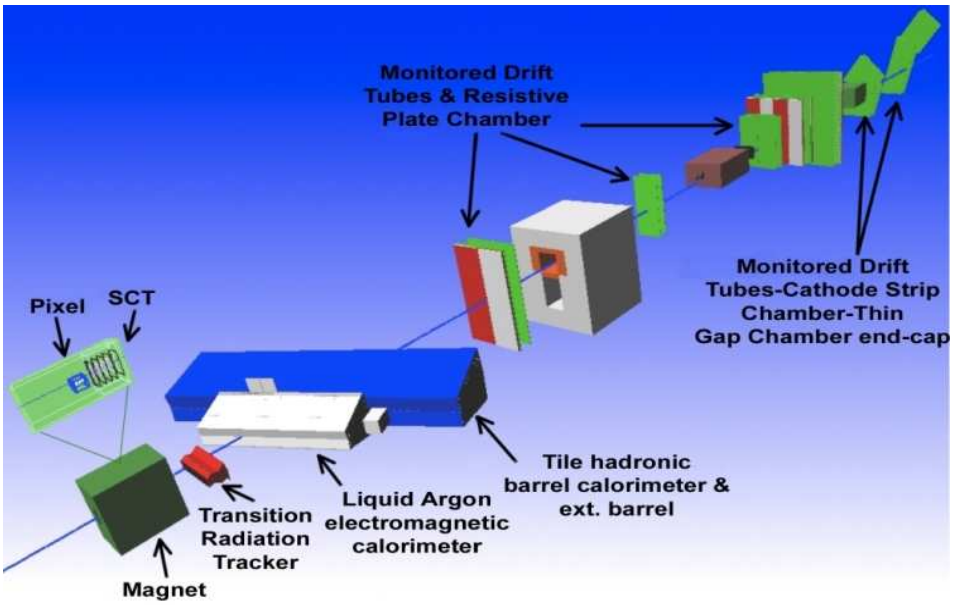

Figure 1: *The CTB layout: the distance between the calorimiter system and the interaction point (assumed to be on the axis of the H8 beam, at the front surface of the Inner Detector magnet) is about* 6 *m, while the beam line intersects the first muon barrel chamber about* 34 *m away from the interaction point.*

1.1 Calorimeter system

The LAr module and the three Tilecal modules were placed on a common table that could rotate and translate in such a way the beam could hit a specific η cell (Figure 2). The Tilecal modules were in contact (with an air gap of 28 *mm*) with the LAr cryostat and they were 1942 *mm* long. The Tile modules were radially segmented (along the beam direction) into three layers (or samples) corresponding, at $\eta = 0$, to 1.4, 3.9 and 1.8 hadronic interaction lengths respectively. The LAr module was divided into three radial samples as well for a total of 24 X_0 at $\eta = 0$.

1.2 Muon set-up

The muon system set-up (Figure 3) included a full barrel tower (six MDT chambers − two BILs, two BMLs and two BOLs −, four BML and two BOL RPCs) and an end-cap octant (six MDT chambers - two EIs, two EMs and two EOs -, three TGCs and one CSC). In addition one BIL chamber on a rotating support was installed upstream of the barrel tower. MDT chambers were operated at their nominal conditions: Ar (93%) and CO_2 (7%) mixture at 3 bar absolute pressure with a high voltage of 3080 V.

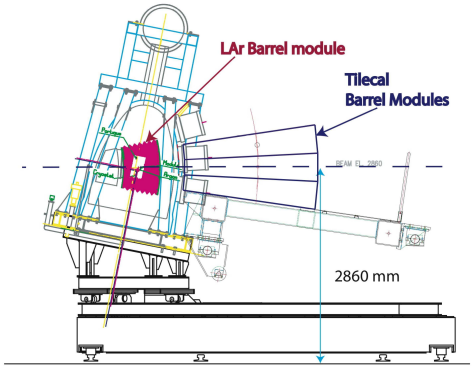

Figure 2: *The calorimiter system layout.*

A two meter long dipole magnet (MBPL) was installed downstream the first BIL chamber, in front of the muon barrel stand with vertical orientation of the field. Another one meter long [2] magnet (MBPS) was installed between the EI and EM stations of the end-cap stand. Magnets were used to steer the beam and allow momentum measurements.

2 Energy loss in calorimeters using muon spectrometer information

In this section a study using the combined information from the muon and calorimeter systems is presented. The main aim of the work is to measure the momentum distribution of muons with large energy loss in the calorimeters and compare results with the `Geant4` [3] based simulation.

2.1 Energy loss of muons in matter

A nice review of formulae and calculations of the muon energy loss in different media can be found in [4]. Muons loose their energy in matter mainly via electromagnetic processes: ionization, bremsstrahlung and direct pair production.

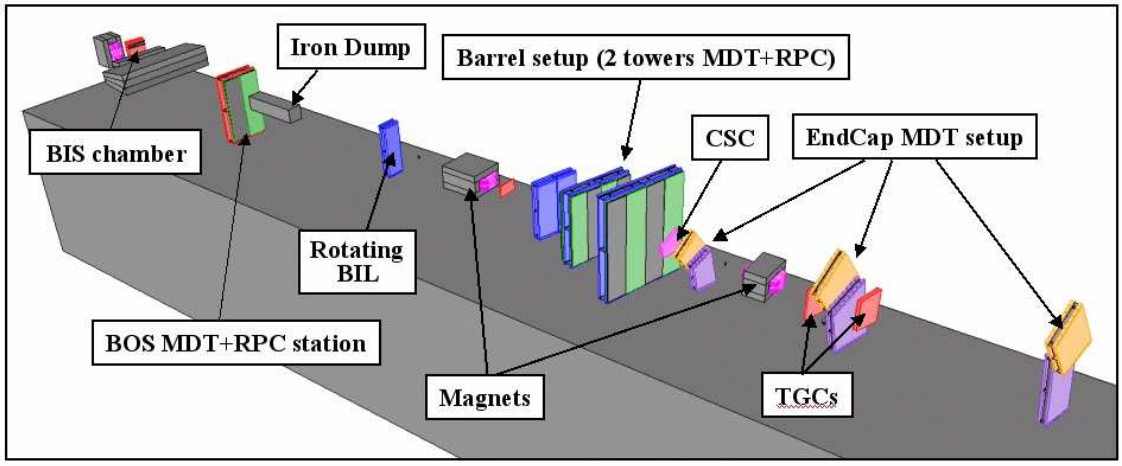

Figure 3: *The muon spectrometer layout: the muon setup starts about* 12 *m away from the interaction point (the BOS MDT chamber placed downstream the calorimeter system). The beam line intersects the BIL station about* 34 *m away from the interaction point and the distance between each MDT barrel station is about* 2 *m. The distance between the EI and the BOL stations is about* 2 *m, and the EM and EO stations are about* 47 *m and* 55 *m away from the interaction point respectively. The BOS and BIS MDT chambers upstream the barrel stand were used for specific calorimeter studies.*

2.1.1 Ionization

The energy loss of a muon with energy E due to ionization is described by the Bethe-Bloch formula

$$\frac{dE}{dx} = \alpha^2 2\pi N \lambda_e^2 \frac{Z m_e}{A\beta^2} \left\{ \ln \frac{2m_e \beta^2 \gamma^2 E'_m}{I^2(Z)} - 2\beta^2 + \frac{E'^2_m}{4E^2} - \delta \right\}$$

where α is the fine structure constant, N is Avogadro's constant, Z and A are the atomic and mass number of the traversed medium, λ_e is the electron Compton wavelength, $I(Z)$ is the mean ionization potential of the medium, E'_m is the maximum energy transferable to the electron and δ is the density correction [5].

2.1.2 Bremsstrahlung

The cross-section for muon bremsstrahlung has been computed by Petrukhin an Shestakov [6] and can be written as

$$\frac{d\sigma}{dv} = \alpha^3 \left(2Z\lambda_e \frac{m_e}{m_\mu} \right)^2 \frac{1}{v} \left(\frac{4}{3} - \frac{4}{3}v + v^2 \right) \phi(\delta)$$

where v is the fraction of energy transferred to the photon. The approximation for $\phi(\delta)$ can be found in [6]. The mean energy loss due to bremsstrahlung can be calculate solving the integral

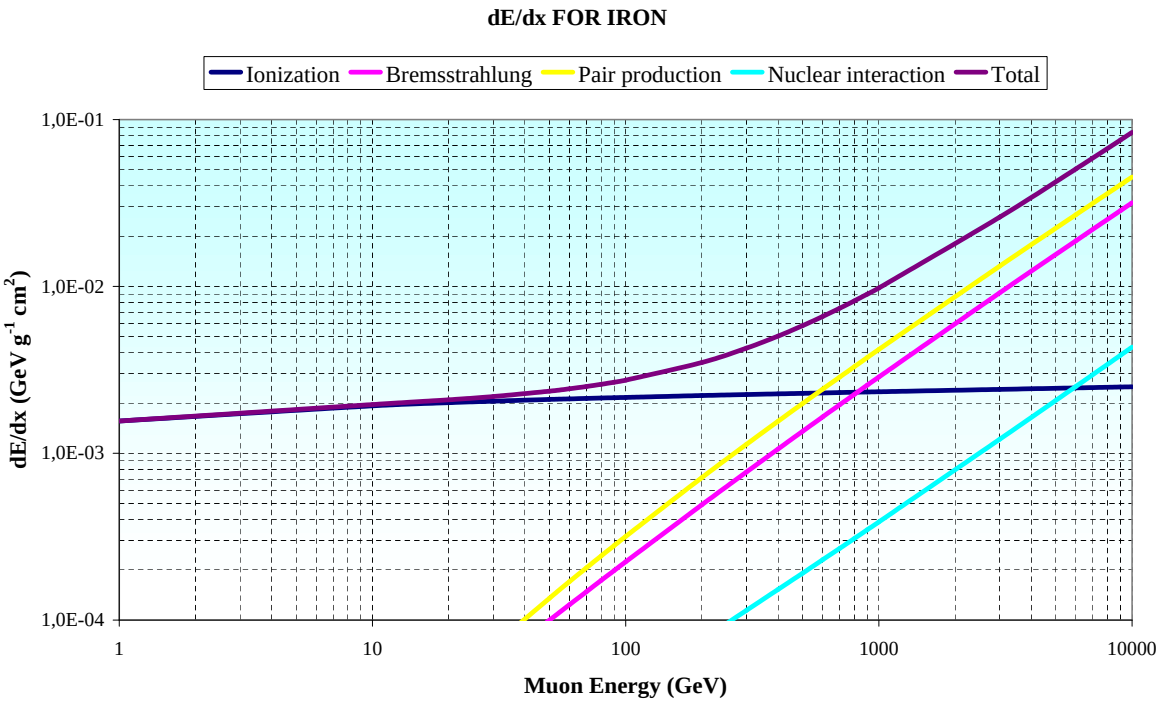

Figure 4: *Muon energy loss in iron: the different contributions to the energy loss are shown. The term corresponding to photonuclear interactions is well described in [4].*

$$\frac{dE}{dx} = E\frac{N}{A}\int_{v_{\min}}^{v_{\max}} v\frac{d\sigma}{dv}dv$$

between $v_{\min} = 0$ and $v_{\max} = 1 - \frac{3Z^{1/3}m_\mu}{4E}\sqrt{e}$.

2.1.3 Direct electron pair production

The direct pair production coss-section was parametrized by Kokoulin and Petrukhin using a QED calculation [7] and it can be expressed as

$$\frac{d^2\sigma}{dvd\rho} = \alpha^4\frac{2}{3\pi}\left(Z\lambda_e\right)^2\frac{1-v}{v}\left(\phi_e + \frac{m_e^2}{m_\mu^2}\phi_\mu\right)$$

where $\rho = \frac{E^+ - E^-}{E^+ + E^-}$ is the asymmetry parameter of the electron-positron pair and ϕ_e and ϕ_μ correspond to different QED diagrams [8]. The energy loss due to pair production can be calculated solving the integral

$$\frac{dE}{dx} = 2E\frac{N}{A}\int_{v_{\min}}^{v_{\max}} v\int_0^{\rho_{\max}}\frac{d^2\sigma}{dvd\rho}d\rho dv$$

Figure 4 shows the different contributions to the muon energy loss as computed in [4]. How these electromagnetic processes are implemented by the `GEANT4` simulation toolkit can be found in [9].

2.2 Data samples

Processed data samples (about 250000 events) refer to combined runs taken in November 2004. The beam was made up of pions with an energy of 350 GeV. The trigger assertion was given by the coincidence of signals coming from two scintillating counter systems: the first one, upstream the Inner Detector region, covered an area of 3×3 cm^2, while the second one, in the muon region, was made up of two 10×10 cm^2 scintillators. The trigger allowed to select muons (as products of the pion decay) among a large number of pions. Calorimeters were placed at $\eta \sim 0.55$. The muon momentum was measured by the deflection angle in the magnetic field of the MBPS dipole.

2.3 Muon momentum measurement

The muon momentum was measured comparing the muon track angle in the end-cap stand in runs with the magnet switched on and off. Using this method the momentum was computed as

$$P(GeV) = \frac{0.3BL(Tm)}{\Delta\theta}$$

being $\Delta\theta = \Delta\alpha_{B\neq 0} - \Delta\alpha_{B=0}$ the difference between the track angle in the EM-EO end-cap and in the BOL-BIL barrel chambers with the magnet switched on and off respectively. The BL value was 2 Tm. Assuming a $\Delta\theta$ resolution of about 200 μrad then a momentum resolution of about 20 GeV was expected. The measured muon momentum distribution is shown in Figure 5: the range of momentum values was compatible with the expected energy of muons decaying from ~ 350 GeV pions.

2.4 Simulation procedure

The simulation was performed using the CTB_G4Sim [10] package in the ATHENA [11] framework. Events were produced following some simple rules:

- A muon beam was generated with an energy profile tuned on experimental data;
- Only calorimeter signals were simulated: we were only looking at the particle energy and momentum *after* the calorimeters (*i.e.,* in the muon spectrometer) and at the energy loss (E_{loss}) *in* calorimeters;
- Calorimeters were put at $\eta \sim 0.55$ as in the real set-up to be sure that particles crossed the same amount of material.

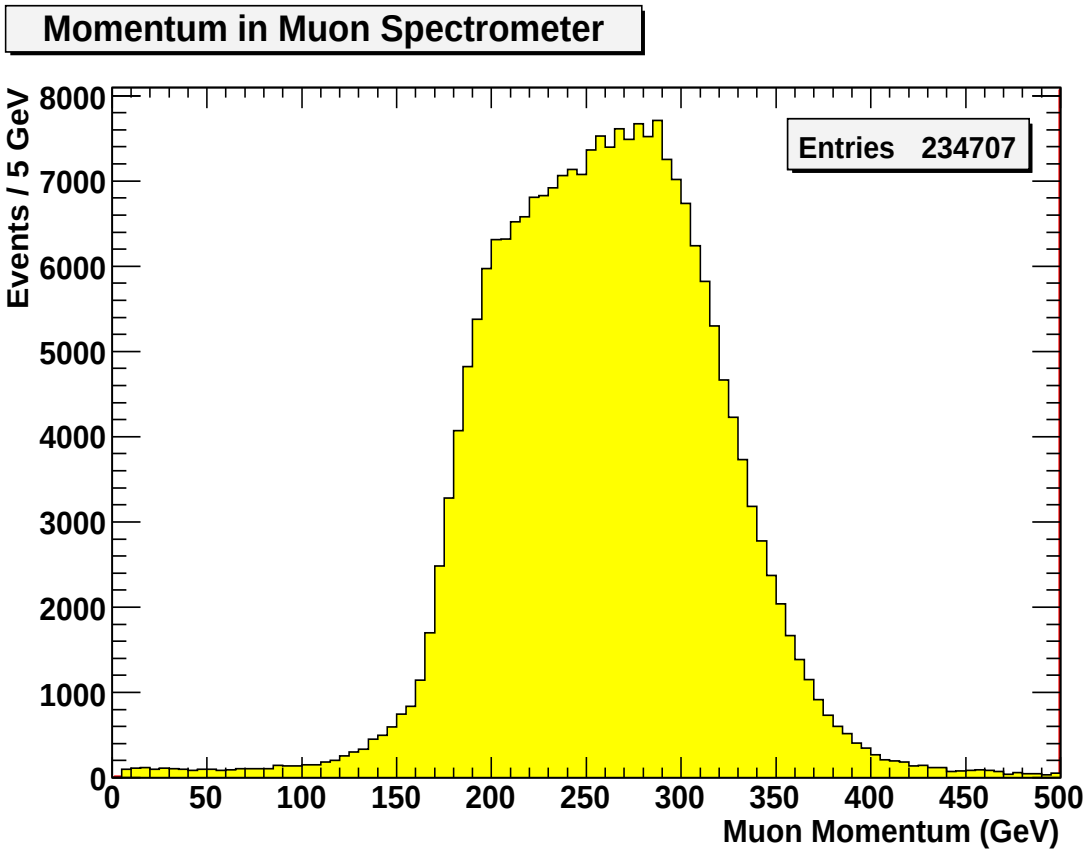

Figure 5: *Muon momentum measured in muon spectrometer.*

2.4.1 Beam energy profile

The first step in simulation was to generate a beam energy profile similar to the one observed in experimental data. The muon momentum spectrum shown in Figure 5 was used to generate muons with the correct energy distribution.

Figure 6 shows the comparison between experimental and simulated energy profiles. Since the muon momentum was measured downstream the calorimeter system and the beam E_{loss} before the muon spectrometer had to be guessed at the particle generation level, a little shift between the two distributions can be noticed.

2.4.2 LAr and Tile response

To test the goodness of the calorimeter response a topological clustering algorithm was used to reconstruct the muon E_{loss} both in LAr and Tile. The algorithm groups calorimeter cells in clusters based on their neighbor relations and on the significance of their energy contents.

As shown in Figure 7 the distribution of the difference between the Tile and LAr response and the true total E_{loss} had a mean value of $\sim 500\ MeV$ and an RMS of $\sim 1\ GeV$. This small shift was considered as negligible with respect to the energy

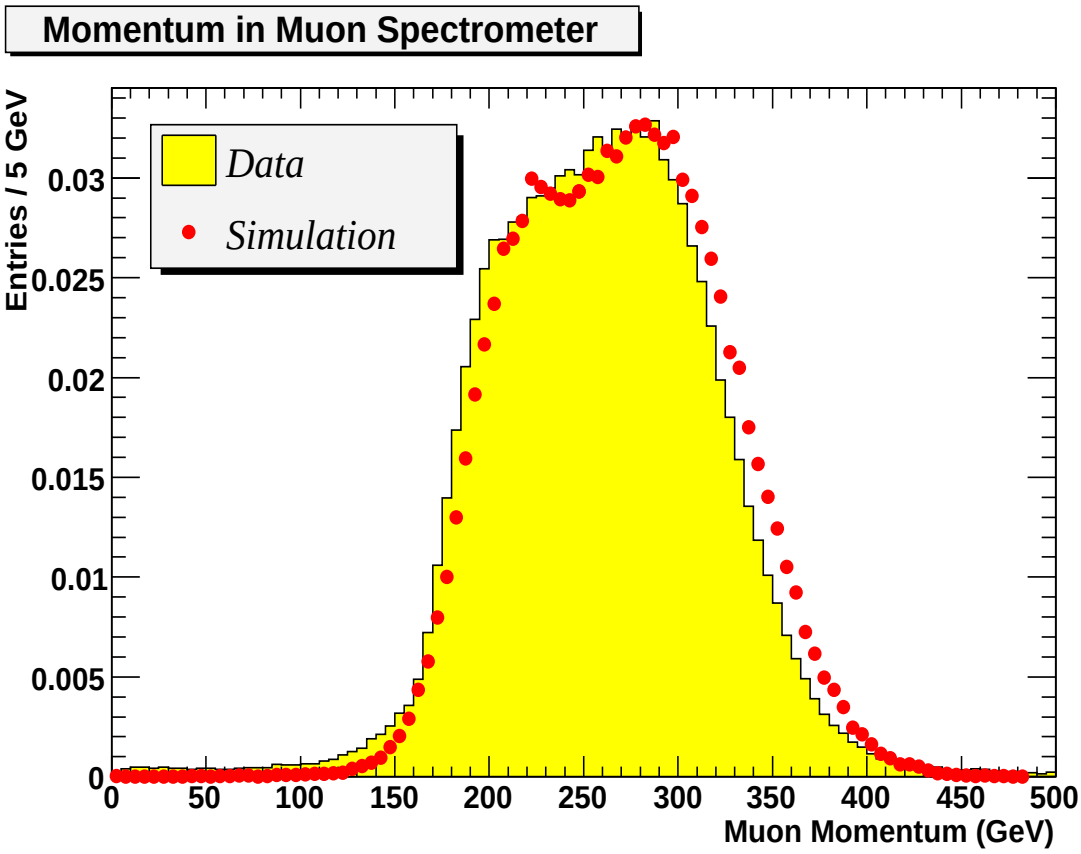

Figure 6: *Muon momentum spectrum in the spectrometer for measured and simulated data. Both distributions were normalized to the same number of events.*

scale relevant for this study and therefore the topological clustering was used in this analysis.

Figure 8 shows the muon E_{loss} as a function of the muon energy: as expected from the brief excursus in Section 2.1, greater the beam energy greater the energy released in calorimeters.

2.5 Experimental data and simulation comparison

In the data analysis two main cuts were applied to accept an event:

- A good track had to be reconstructed in the muon spectrometer. This criterion ensured the selection of muon events.
- The E_{loss} in both electromagnetic and hadronic calorimeters had to be greater than zero. This cut was useful to remove the calorimeter noise.

Figure 9 shows the energy in LAr and Tile as a function of η and ϕ of cells: the signal due to the passage of particles is clearly visible over a flat noise. Then

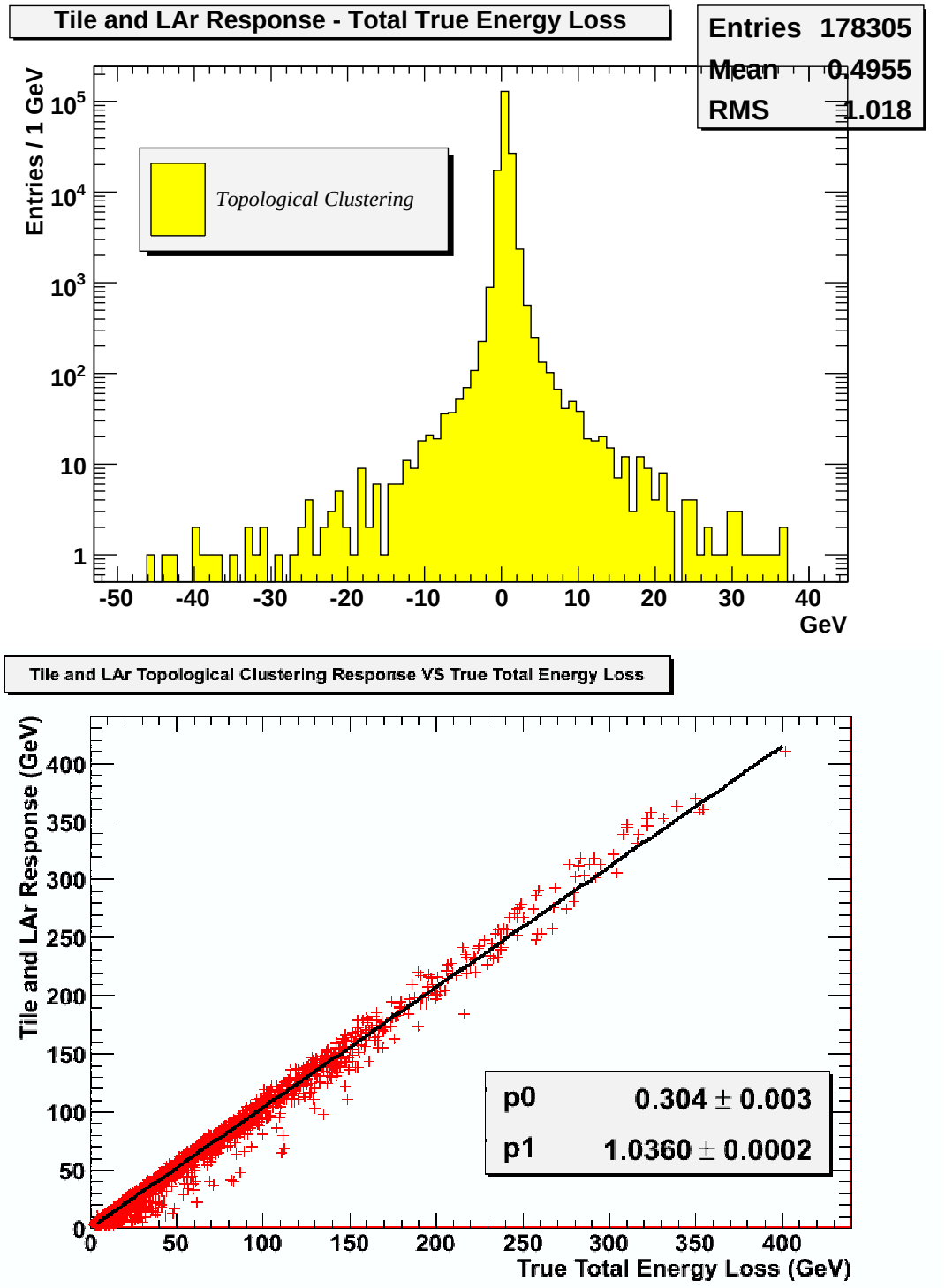

Figure 7: *Distribution of the difference between LAr+Tile response and true energy loss (up) and calorimeter response as a function of the true energy loss (down). Data points were fitted with a first degree polynomial.*

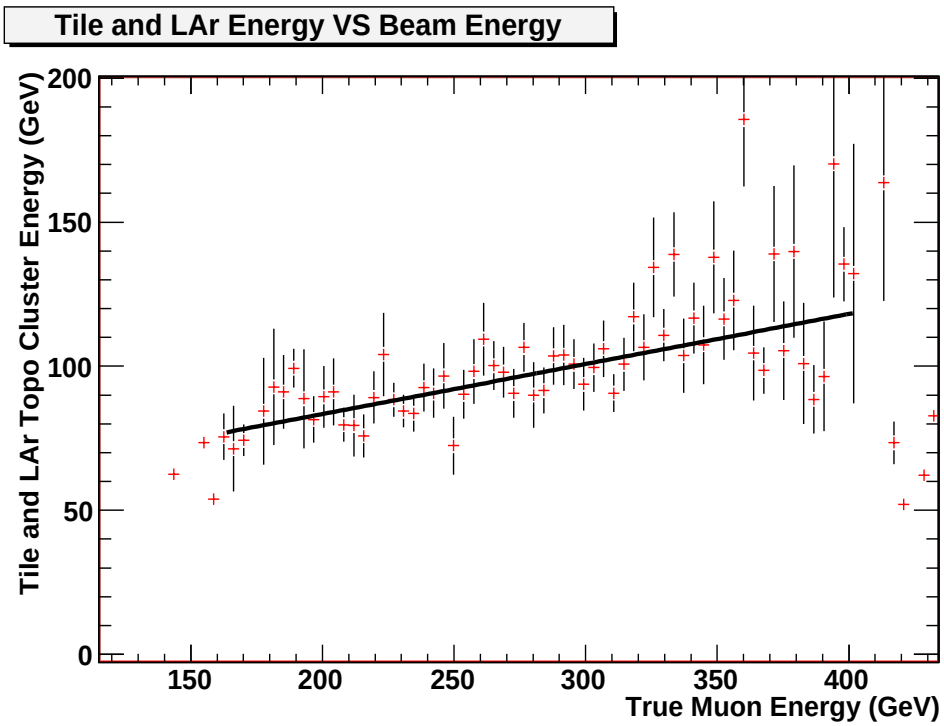

Figure 8: *Energy loss as a function of muon energy from simulation for events with* $E_{loss} > 50\ GeV$.

for selected events the E_{loss} was computed applying the same algorithm used for simulated data (topological clustering).

A first comparison between experimental and simulated data E_{loss} distributions showed a poor agreement. Figure 10 shows an excess of events with high E_{loss} present in experimental data with respect to the simulated data both for LAr and Tile.

A first attempt to understand the nature of the difference between experimental and simulated data was to look at the correlation between the E_{loss} in calorimeters and the muon momentum measured in the muon spectrometer. A clear difference between simulation (Figure 11.1) and experimental data (Figure 11.2) was due to events with large E_{loss} and large momentum in the spectrometer (of the order of $\sim 300\ GeV$).

A simple hypothesis was to tag these events as the cause of the large E_{loss} overabundance present in experimental data. To understand the meaning of this signature the same plot as in Figure 11.2 was produced for each of the three Tile radial layers (Figure 12). The plot referring to the third layer (Figure 12.3) demonstrated a correlation much more similar to what observed in simulated events (Figure 11.1) than the one referring to the fist layer (Figure 12.1), even if both layers had almost the same hadronic interaction lengths. This was the proof that almost the whole energy overabundance was contained in the first two Tile layers. This evidence lead to the assumption of an accidental pion contamination in the selected events.

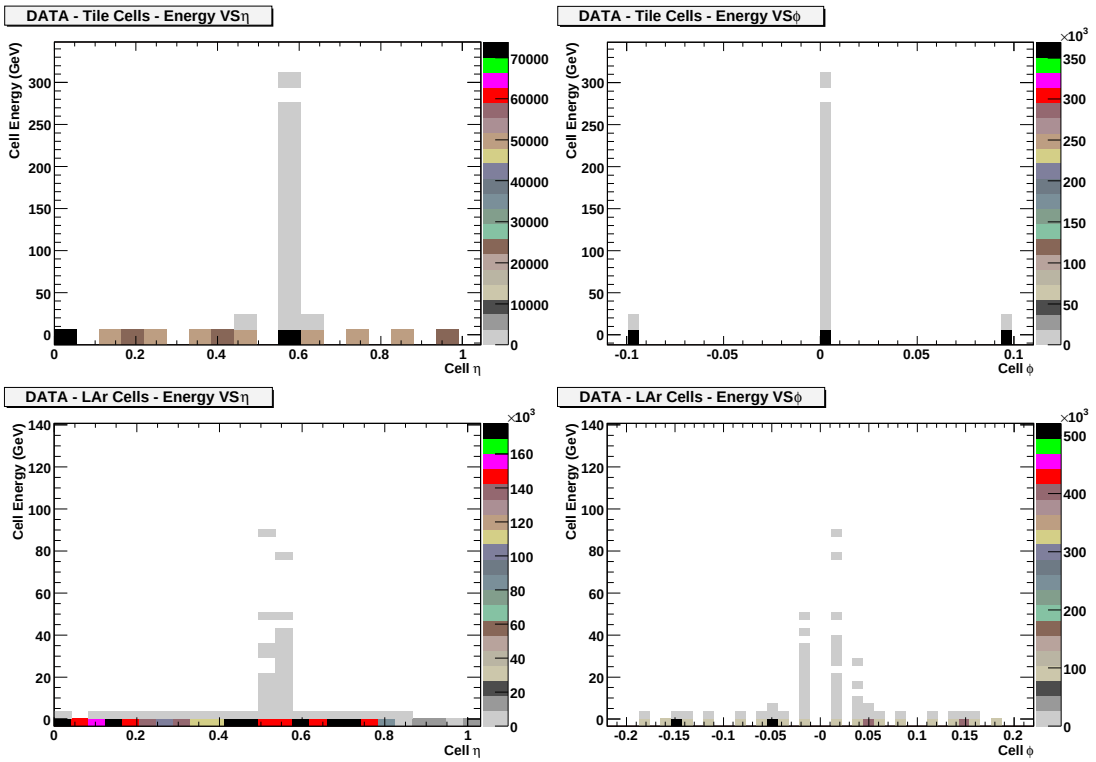

Figure 9: *Energy in Tile (up) and LAr (down) as a function of cell η (left) and ϕ (right).*

In fact, since the beam had a very large pion component, the probability to have an accidental pion contamination in the data was not negligible. To have an estimate of the pion component in the beam, the 3×3 cm^2 scintillating counter rate (*i.e.* the particle rate before the calorimeter system, mainly pions) was about 100 KHz, while the 10×10 cm^2 scintillating counter measured a rate of about 10 KHz (*i.e.* the particle rate after the calorimeter system, mainly muons). Taking into account an integration window of 100 ns for the Tile the probability to have an accidental pion contamination could be computed as

$$p = \frac{1}{\tau} \int_0^{t_1} e^{-\frac{t}{\tau}} dt \sim \frac{t_1}{\tau} = 0.01$$

where $\tau \sim 10^{-5}$ s and $t_1 = 10^{-7}$ s. This value was in agreement with the fraction of events (0.9%) characterised by both E_{loss} and $Momentum$ between 200 and 350 GeV.

2.6 Single muon event selection

The procedure to reject accidental pions was based upon two assumptions:

- The probability for a muon to have a large energy loss due to bremsstrahlung or pair production in more than one Tile radial layer is very small;

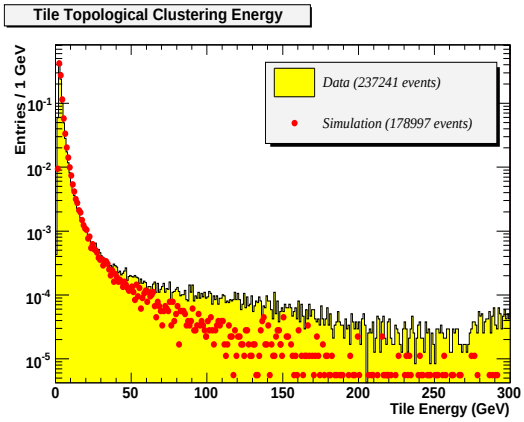

10.1: Energy loss in Tile

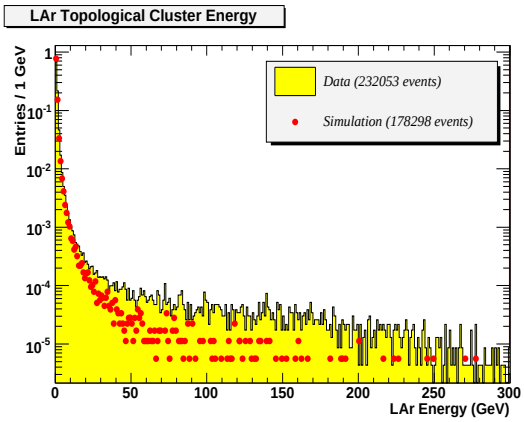

10.2: Energy loss in LAr

Figure 10: *Tile (10.1) and LAr (10.2) E_{loss} distributions for experimental and simulated data. Histograms were normalized to the same number of events (the reported number of entries refers to the histograms before the normalization).*

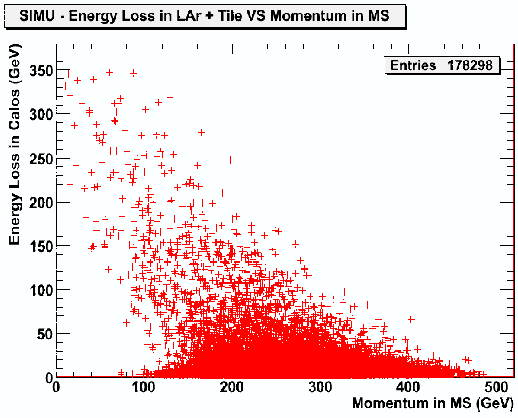

11.1: Simulation

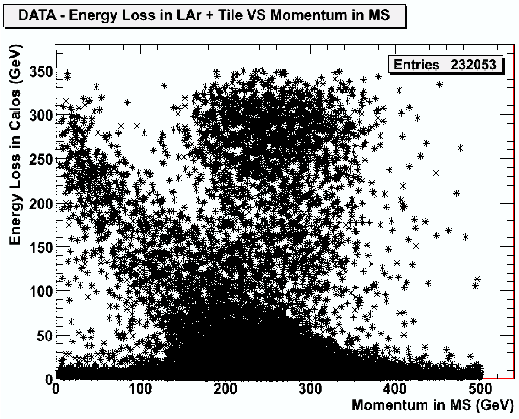

11.2: Real data

Figure 11: *Scatter plots showing the correlation between the E_{loss} in calorimeters and the muon momentum measured in the muon spectrometer for simulated (11.1) and experimental data (11.2).*

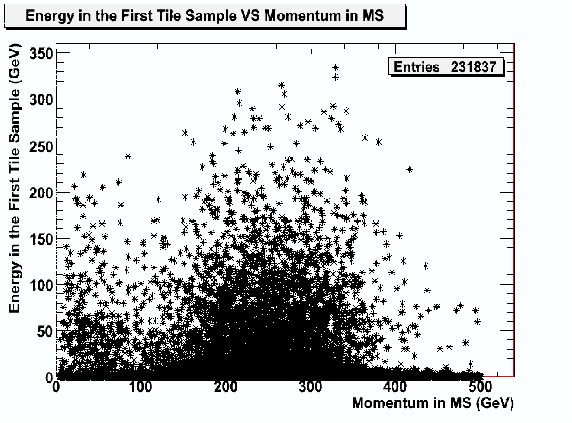

12.1: First Tile sample

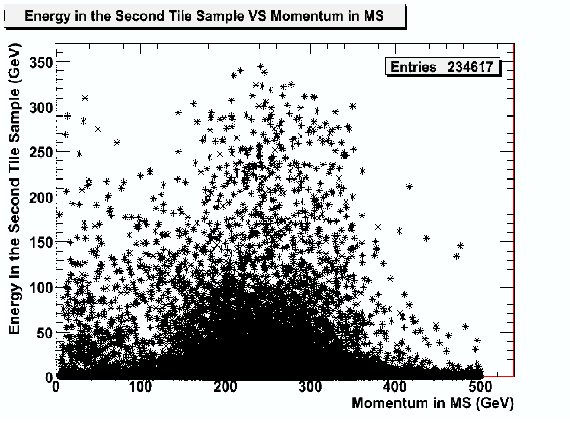

12.2: Second Tile sample

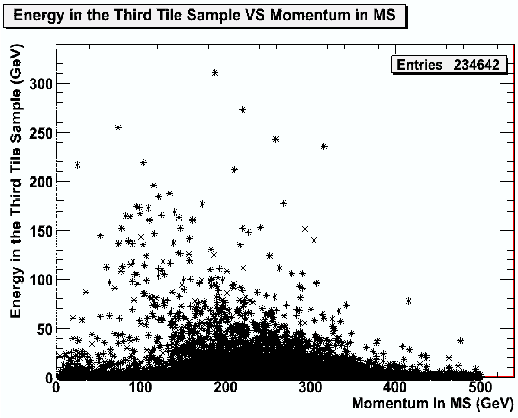

12.3: Third Tile sample

Figure 12: *Experimental data: scatter plots showing the correlation between the E_{loss} in each Tile radial layer and the muon momentum measured in the muon spectrometer.*

- The muon energy loss due to bremsstrahlung or pair production is well contained within a single Tile radial layer (each layer corresponding to many electromagnetic radiation lengths).

Following this hypothesis only events with a Minimum Ionizing Particle (MIP) at least in two out of the three Tile samples were selected. The MIP energy cut was of 1 GeV in the first and third Tile sample and of 2 GeV in the second sample. Figure 13 shows the E_{loss} distribution in the experimental data for each Tile sample.

The application of this selection criterion let the correlation between the E_{loss} in calorimeters and the muon momentum measured in the muon spectrometer agree with simulation prediction as shown in Figure 14.

An independent proof that for some events not only muons were crossing the calorimeter system was given by the peak value of the E_{loss} distribution in LAr (Figure 15). The most probable value of the Landau distribution used to fit the data

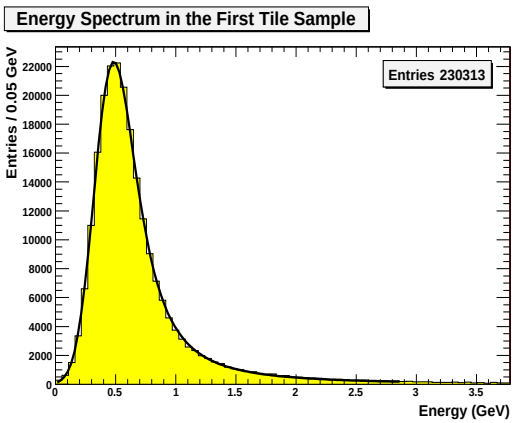

13.1: First Tile sample

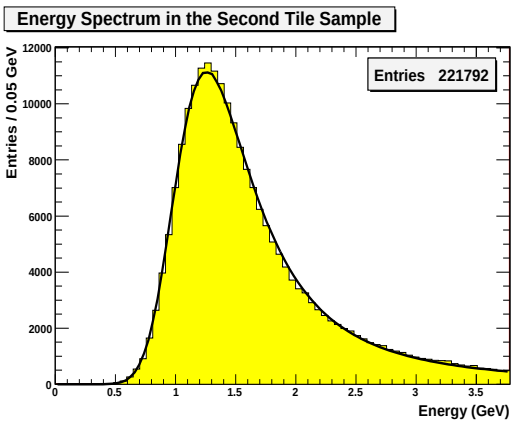

13.2: Second Tile sample

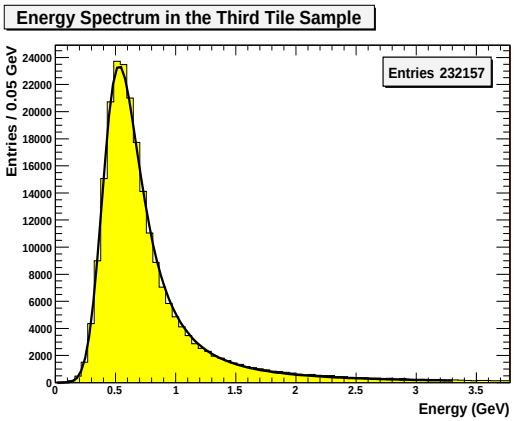

13.3: Third Tile sample

Figure 13: *E_{loss} distribution in each Tile radial layer. Histograms were fitted using a Landau curve and gaussian convolution.*

was (0.604 ± 0.001) GeV for single muon selected events, while it was (1.06 ± 0.06) GeV for accidental pion contaminated events. It was evident that on average for pion contaminated tagged events more than one MIP crossed the LAr calorimeter.

Another hint demonstrating the accidental pion contamination was suggested by the correlation between the LAr and Tile E_{loss} before and after the single muon event selection cut (Figure 16). The application of single muon event criterion granted for the acceptance of events with no pions showering in calorimeters.

After applying the single muon event selection cut a new comparison between experimental and simulated data E_{loss} distributions was done (Figure 17). The agreement between data and simulation became very good as demonstrated by the fraction of events in different E_{loss} bins reported in Table 1.

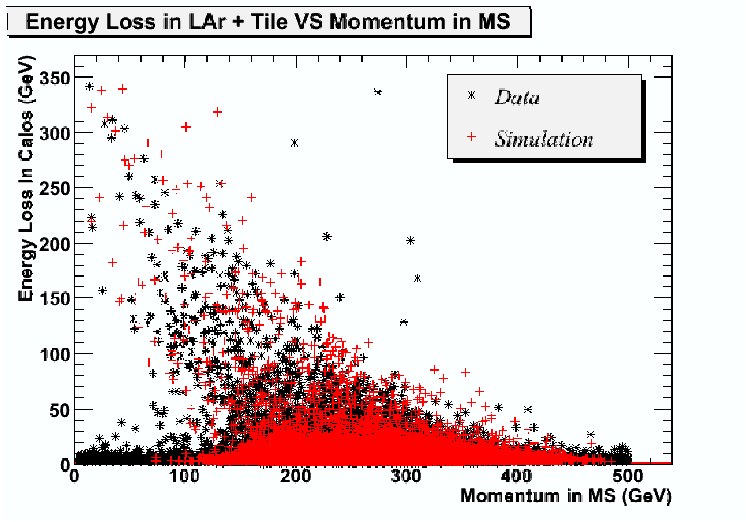

Figure 14: *Correlation between the E_{loss} in calorimeters and the muon momentum measured in the muon spectrometer for experimental and simulated data after single muon event selection cut.*

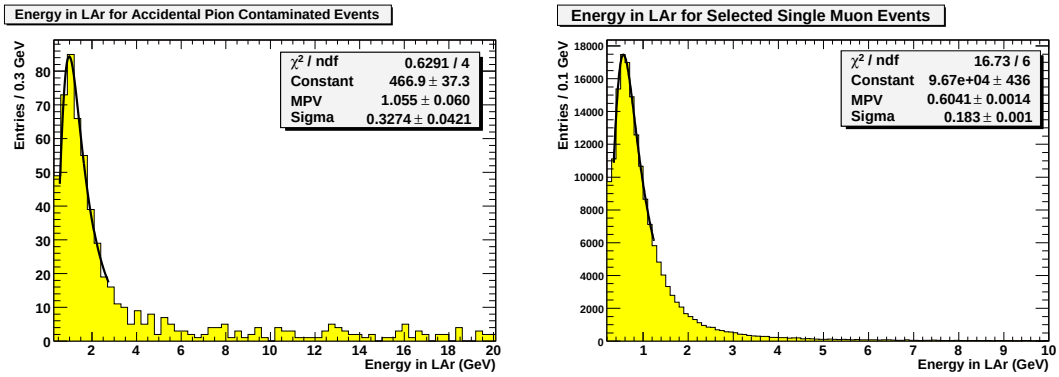

Figure 15: *Energy loss distribution in LAr for two different populations of events: "pion" events (i.e., events with both total E_{loss} and mometum in the muon spectrometer between 200 and 350 GeV) and single muon events. Histograms were fitted with a Landau distribution.*

Energy Range (GeV)	Event Fraction (%)	
	Data	Simulation
$0-10$	96.67 ± 0.04	96.71 ± 0.05
$10-50$	3.06 ± 0.04	3.01 ± 0.04
$50-100$	0.18 ± 0.01	0.17 ± 0.01
>100	0.088 ± 0.006	0.101 ± 0.008

Table 1: *Fraction of events belonging to some E_{loss} bins for experimental and simulated data.*

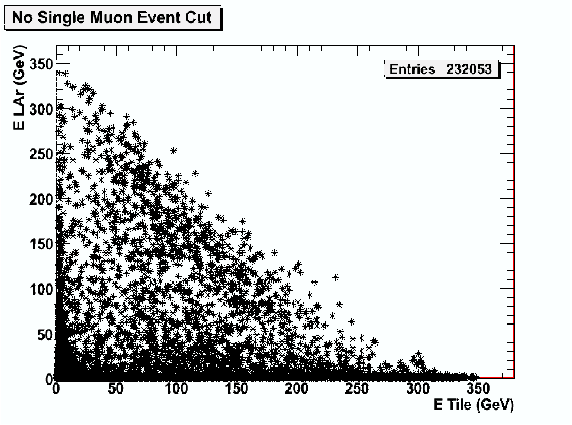

16.1: No single muon selection cut applied

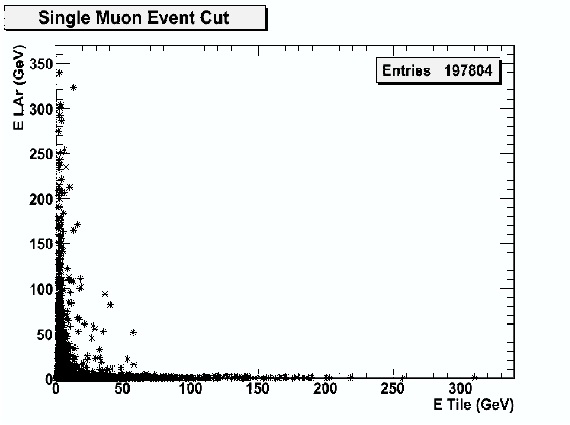

16.2: Single muon selection cut applied

Figure 16: *Correlation between the E_{loss} in LAr and Tile without (16.1) and with (16.2) the single muon event selection cut applied. In 16.1 a clear pion signature in calorimeters could be noticed.*

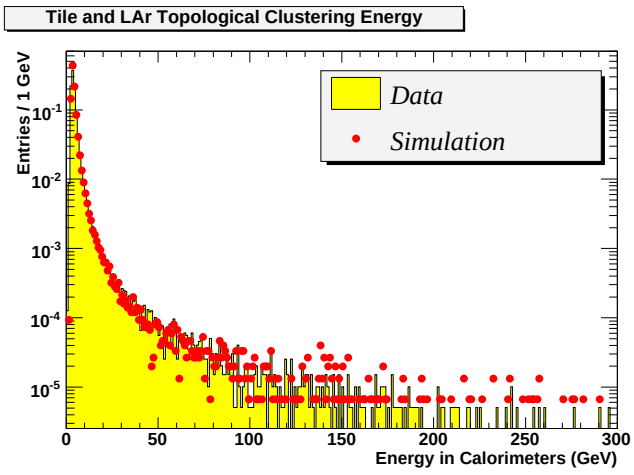

Figure 17: *Tile+LAr E_{loss} distributions for experimental and simulated data. Same cuts were applied in data and simulation. Histograms were normalized to the same number of events.*

3 Conclusions

The fraction of muons with *catastrophic* energy losses in calorimeters has been investigated. Results from experimental data analysis have been compared to a GEANT4 simulation of the calorimeter and muon spectrometer systems. Simulation parameters were tuned on experimental data run conditions. In particular the beam energy profile was correctly reproduced to avoid biases in energy released in calorimeters. Furthermore same reconstruction and analysis algorithms were used both in simulation and for experimental data.

The combined set-up allowed to use the muon spectrometer and calorimeter information to understand an initial disagreement between simulation and experimental data due to an accidental pion contamination. After single muon event selection the probability for a muon to have an energy loss greater than 10 GeV was calculated to be $(3.27 \pm 0.05)\%$ for simulation and $(3.37 \pm 0.05)\%$ for experimental data analysis.

4 Acknowledgements

We would like to thank all the H8 crew and in particular the SPS people for their great work and support during all the test beam period.

References

[1] B. Di Girolamo, M. Gallas, T. Koffas, **ATLAS Barrel Combined Run in 2004 Test Beam Setup and its Evolutions**, EDMS Note ATC-TT-IN-0001, Available as https://edms.cern.ch/file/406980/3/TB2004_layout_v06.pdf

[2] **MBPS magnet characteristics,** Available as https://edms.cern.ch/file/408415/2/mbps.pdf

[3] A. Agostinelli et al, **Geant4 - a simulation toolkit**, Nucl. Inst. Meth. **A 506** (2003), 250-303

[4] W. Lohmann, R. Kopp, R. Woss, **Energy Loss of Muons in the Energy Range 1-10000 GeV**, CERN-85-03

[5] R.M. Sternheimer et al., Atomic Data and Nucl. Data Tables **30** (1984) 261

[6] A.A. Petrukhin, V.V. Shestakov, Can. J. Phys. **46** (1968) S377

[7] R.P. Kokoulin, A.A. Petrukhin, Proc. 11^{th} Int. Conf. on Cosmic Rays, Budapest, 1969, Acta Phys. Hung. **29**, Suppl. 4 (1970) 277

[8] S.R. Kelner, Yu. D. Kotov, SOv. J. Nucl. Phys. **7** (1968) 237

[9] The G4 Physics Reference Manual, available as http://geant4.web.cern.ch/geant4/UserDocumentation/UsersGuides/PhysicsReferenceManual/fo/PhysicsReferenceManual.pdf

[10] Atlas Combined Test Beam Simulation - User Manual, Available as http://atlas.web.cern.ch/Atlas/GROUPS/SOFTWARE/OO/simulation/geant4/CTB_G4Sim/doc/ctb_Umanual.html

[11] ATHENA Developer Guide, Available as http://atlas.web.cern.ch/Atlas/GROUPS/SOFTWARE/OO/architecture/General/Tech.Doc/Manual/2.0.0/DRAFT/AthenaUserGuide/pdf